JOURNAL OF VIROLOGY, June 2000, p. 5509–5515 Vol. 74, No. 6
0022-538X/00/$04.00+0

Interactions between Hepatitis Delta Virus Proteins

GLORIA MORALEDA,[1] KATE DINGLE,[1] PREETHA BISWAS,[1] JINHONG CHANG,[1] HARMON ZUCCOLA,[2] JAMES HOGLE,[2] AND JOHN TAYLOR[1]*

Fox Chase Cancer Center, Philadelphia, Pennsylvania 19111-2497,[1] and Harvard Medical School, Boston, Massachusetts 02115[2]

Received 15 December 1999/Accepted 9 March 2000

The 195- and 214-amino-acid (aa) forms of the delta protein (δAg-S and δAg-L, respectively) of hepatitis delta virus (HDV) differ only in the 19-aa C-terminal extension unique to δAg-L. δAg-S is needed for genome replication, while δAg-L is needed for particle assembly. These proteins share a region at aa 12 to 60, which mediates protein-protein interactions essential for HDV replication. H. Zuccola et al. (Structure 6:821–830, 1998) reported a crystal structure for a peptide spanning this region which demonstrates an antiparallel coiled-coil dimer interaction with the potential to form tetramers of dimers. Our studies tested whether predictions based on this structure could be extrapolated to conditions where the peptide was replaced by full-length δAg-S or δAg-L, and when the assays were not in vitro but in vivo. Nine amino acids that are conserved between several isolates of HDV and predicted to be important in multimerization were mutated to alanine on both δAg-S and δAg-L. We found that the predicted hierarchy of importance of these nine mutations correlated to a significant extent with the observed in vivo effects on the ability of these proteins to (i) support in *trans* the replication of the HDV genome when expressed on δAg-S and (ii) act as dominant-negative inhibitors of replication when expressed on δAg-L. We thus infer that these biological activities of δAg depend on ordered protein-protein interactions.

Human hepatitis delta virus (HDV) is a satellite virus of hepatitis B virus (HBV) and requires HBV envelope proteins for packaging, secretion and infection (reviewed in reference 24). HDV particles contain a ribonucleoprotein core composed of the circular 1.7-kb RNA genome and multiple copies of the only HDV-encoded protein, delta antigen (δAg) (23). There are two forms of the δAg. The first is a 195-amino-acid (aa) species, known as the small delta protein (δAg-S), which is essential for replication of the RNA genome (11). The second is 19 aa longer at its C terminus (δAg-L) and arises as a consequence of a posttranscriptional RNA editing event (17). This δAg-L is a dominant-negative inhibitor of genome replication (4), but it is essential for particle assembly (2).

These two δAg species share 195 aa of primary sequence and thus have some common features. These include (i) a coiled-coil domain located at aa 12 to 60, which facilitates protein-protein interactions (21); (ii) a bipartite nuclear localization signal, between aa 68 and 88 (28); and (iii) a bipartite RNA-binding domain, consisting of aa 97 to 107 and 136 to 146 (3).

The coiled-coil domain has been shown to be required for a number of the functions of both small and large delta antigens. (i) Mutations that destroy or alter this dimerization domain reduce or eliminate the ability of δAg-S to function as a *trans* activator of HDV replication (15). (ii) These same mutations when presented on δAg-L prevent the antigen from inhibiting HDV RNA replication and also block the ability to coassemble δAg-S into viral particles (15).

Biophysical studies by Rozzelle et al. showed that the synthetic peptide that corresponds to aa 12 to 60 of δAg was α helical in structure and was sufficient for dimerization and even multimerization (21). Recently, Zuccola et al. solved the crystal structure for this peptide and confirmed that it contains a long N-terminal and a short C-terminal α-helical segment separated at aa 49 by proline (29). To form a dimer, the long helices of each of two monomers wrap around each other, forming an antiparallel coiled-coil (29). In addition, each dimer associates with three other dimers, forming what has been called a "doughnut-like octamer" (29). In support of this model, they used recombinant δAg-S, and chemical cross-linking followed by mass spectrometry, to show that octamers could form in vitro. Finally, based on the alignment of several different δAg sequences of this region, they noted that certain amino acids were both conserved and predicted to be important for dimerization and/or multimerization. Based on their study, we have selected nine such critical amino acids and evaluated their importance in the context of both full-length δAg-S and δAg-L. Each of these single amino acids was changed to alanine in order to avoid altering the secondary structure of the protein while disrupting the intermolecular associations. This series of δAg mutants was then evaluated by in vivo assays to determine whether they still (i) supported HDV replication, (ii) acted as dominant-negative inhibitors, (iii) had the ability to coassemble into particles, (iv) made complexes with an affinity-tagged form of δAg-S, and (v) were able to increase the accumulation of processed HDV RNA species. We consider that the results of (i), (ii), and to some extent (iv) are supportive of the predictions based upon the crystal structure, while those of (iii) reveal the diversity and complexity of δAg interactions in vivo and those of (v) indicate separate functions that are independent of such interactions.

MATERIALS AND METHODS

Plasmids. Most constructs were based on the vector pSVL (Pharmacia). pTW148 expresses 1.2× unit-length HDV cDNA and has a frameshift in the δAg-S open reading frame; thus, HDV replication can be achieved only by supplying δAg-S in *trans* (26). pDL444 and pDL445 were used to express the wild-type δAg-S and δAg-L, respectively (15). Plasmids pDL448 and pDL449 express δAg-S(Δ19–31) and δAg-L(Δ19–31), respectively, that have a deletion of 13 aa from the coiled-coil region (15). pDL480 expresses antigenomic HDV RNA with a deletion spanning the region between nucleotides 215 and 1380 (14). The following constructs were based on the vector pcDNA3 (Invitrogen). Constructs pPB102 and pPB105 express δAg-S(Δ19–31) and δAg-S(FLAG), respectively. The latter species is a form of δAg-S with the FLAG epitope (Asp-Tyr-

* Corresponding author. Mailing address: Fox Chase Cancer Center, 7701 Burholme Ave., Philadelphia, PA 19111-2497. Phone: (215) 728-2436. Fax: (215) 728-3105. E-mail: jm_taylor@fccc.edu.

Lys-Asp-Asp-Asp-Asp-Lys) at the N terminus. Plasmids pTW198 and pTW199 express wild-type δAg-S and δAg-L, respectively.

Construction of plasmids expressing δAg-S and δAg-L with amino acid substitutions in the coiled-coil region. To construct mutated plasmids, primers containing the sequences corresponding to the amino acid substitution were used to amplify that part of the δAg corresponding to aa 9 to 58, numbered according to the sequence of Kuo et al. (11). The PCR fragments were then inserted between the *Eco*RI and *Sac*II sites of pDL444 or pDL445 to get the mutated forms of δAg-S and δAg-L, respectively. All mutants were confirmed by nucleotide sequencing.

DNA transfections. For all experiments, transfection of the human hepatoma cell line Huh7 (20) was performed using FuGENE 6 (Roche) following the manufacturer's instructions.

RNA analysis. Total cell RNA was isolated with Tri Reagent (Molecular Research Center), glyoxalated, and analyzed electrophoretically on gels of 1.7% agarose as previously described (15). RNA was transferred to a nylon membrane (Zeta-probe GT; Bio-Rad) and immobilized by UV cross-linking. Hybridization was performed with ^{32}P-labeled RNA probe specific for antigenomic HDV RNA. Levels of antigenomic RNA were detected and quantitated using a Bio-Imaging system (Fuji).

Protein analysis. Samples were resuspended in Laemmli buffer (13) and analyzed by sodium dodecyl sulfate–12.5% polyacrylamide gel electrophoresis (SDS-PAGE). Proteins were electrotransferred to a nitrocellulose membrane, and δAg was detected by using a rabbit polyclonal antiserum and by incubation with ^{125}I-labeled protein A (Du Pont). Quantitation was via a Bio-Imaging system.

Coassembly of δAg into virus-like particles. Huh7 cells were transfected with plasmid pSV45H (from Don Ganem) for the expression of all three HBV envelope proteins, along with the appropriate plasmids expressing wild-type or mutant forms of δAg-S and δAg-L. Tissue culture medium was collected at 4, 6, and 8 days after transfection and clarified by low-speed centrifugation for 10 min. Then virus-like particles were collected through a 20% sucrose cushion containing 100 mM NaCl, 10 mM Tris-HCl (pH 7.5), and 1 mM EDTA by centrifugation for 18 h at 23,000 rpm in a Beckman SW28 rotor at 4°C. The pellet was analyzed for delta proteins as described above.

Immunoaffinity purification of δAg complexes. Huh7 cells were cotransfected with (i) pPB105, which expresses δAg-S(FLAG), and (ii) pPB102, which expresses δAg-S(Δ19–31), with a deletion in the coil-coiled domain (15), in combination with (iii) wild-type or mutant forms of δAg-S or δAg-L, as indicated in Fig. 6. At 5 days after transfection, we used a modification of the method described by Chiang et al. (5) to purify complexes containing the FLAG epitope. About 10^6 cells were resuspended in 1 ml of 100 mM KCl in BC buffer (20 mM Tris-HCl [pH 7.9], 20% glycerol, 0.2 mM EDTA, 0.5 mM phenylmethylsulfonyl fluoride, 10 mM 2-mercaptoethanol) plus 0.1% NP-40 and then lysed by sonication (five times for 30 s each, at microtip setting) on ice with a 550 Sonic Dismembrator (Fisher Scientific). After clarification for 5 min at 1,500 rpm, one-third of the supernatant was incubated with 50 μl of anti-FLAG M2-agarose (Sigma), which contains the anti-FLAG M2 monoclonal antibody conjugated onto the agarose, at 4°C for 16 h with rotation. After being washed four times in BC300 (BC buffer including 300 mM KCl) plus 0.1% NP-40, once in BC100 (BC buffer containing 100 mM KCl) plus 0.1% NP-40 and once in BC buffer, the bound protein was eluted directly with Laemmli buffer. Aliquots of both total protein and bound protein were subjected to SDS-PAGE and immunoblot analysis as described above.

Accumulation of processed genomic RNA circles in the presence of mutant and wild-type forms of δAg-S. Huh7 cells were cotransfected with plasmid pDL480, to express multimeric HDV RNA, along with a construct expressing one of the δAg-S mutants. Cells were harvested at days 2 and 4 after transfection, and total RNA was assayed by SDS-PAGE and Northern analysis as described above.

RESULTS

Negative controls. For the following in vivo assays of δAg interactions, we used as negative controls specific deleted forms of δAg-S and δAg-L that were unable to dimerize. These mutants, which have a deletion of aa acids 19 to 31, were characterized in the earlier study of Lazinski and Taylor (15). These previous studies showed that (i) both truncated proteins could be stably expressed in Huh7 cells, (ii) δAg-S(Δ19–31) did not support replication, (iii) δAg-L(Δ19–31) could not coassemble wild-type δAg-S, and (iv) δAg-L(Δ19–31) was not a dominant-negative inhibitor. Further studies show that δAg-S(Δ19–31) cannot be coassembled by wild-type δAg-L (data not shown).

Design of δAg mutants. The design was based on a two-step process, essentially as used by Zuccola et al. (29). First, they considered sequence conservation. The sequences of 10 independent HDV isolates were aligned through the region of the delta antigen, and many conserved amino acids were detected.

A

```
12        20          30          40          50          60
 .         .           .           .           .           .
 GREDILEQ WVSGRKKLEE LERDLRKLKK KIKKLEEDNP WLGNIKGIIGK  Makino et al.
 ---E---- --A------- -------T-- -L--I-DE-- --------L--  Kuo et al.
```

B

```
Predicted role in dimerization and multimerization:
     dimerization:       R13, W20, R24, W50, L51
     multimerization:    L17, V21, W50, I54, I57

Predicted rank, in decreasing order of importance in
multimerization:
     R13, W20, W50  >  I54, R24, I57, L17  >  V21, L51
```

C

```
Observed in vivo role of δAg-S in trans support of replication:
     R13, W20, W50, I54, R24, I57  >  L17, V21, L51

Observed in vivo role of δAg-L in dominant-negative inhibition:
     W20, W50  >  R13, I54, R24, I57, L17, V21, L51

Observed in vivo role in formation of complexes with δAg-S(FLAG):
     W50  >  W20, I54, I57  >  R13, L51  >  L17, V21, R24
```

FIG. 1. Predictions and observed consequences of mutating single amino acids of δAg that are both conserved and possibly critical for protein dimerization and/or multimerization. (A) Sequence at aa 12 to 60 of the coiled-coil domain of δAg of Makino et al. (18). Underlined are the amino acids predicted, using the data of Zuccola et al. (29), to be critical for dimerization and/or multimerization. Also shown is the corresponding sequence of δAg from Kuo et al. (12), which is subsequently used as the backbone for the construction of mutant proteins. (B) Individual amino acids that were changed to alanine to test the prediction that they were involved in either dimerization or multimerization. Also shown is a predicted ranking of their importance for multimerization. (C) Mutant proteins organized according to three subsequently observed in vivo distinguishing characteristics (Fig. 3, 4B, and 6) and summarized in Tables 2 and 4.

Second, they used the determined three-dimensional structure to predict which of these conserved amino acids might be needed to maintain dimerization and multimerization. Figure 1A shows two HDV sequences through this region: first, the sequence used for the crystal structure (18); and second, the sequence used for our subsequent in vivo studies (12). Also indicated are the conserved amino acids and the nine individual ones chosen for mutagenesis to alanine. The intent of these substitutions was to maintain the primary and secondary structures while testing the predictions regarding tertiary structure. As summarized in Fig. 1B, we assigned a hierarchy of effects for each of these nine mutations, in terms of their potential role in dimerization and multimerization of δAg.

The rationale for the hierarchy was as follows. Based on the crystal structure of the δAg oligomerization domain, W20, W50, and R13 play essential roles in stabilizing the δAg octamer. W50 is buried within the monomer/monomer interface as well as the dimer/dimer interface. R13 blocks solvent from the hydrophobic core at both the monomer/monomer interface and dimer/dimer interface. W20 not only is buried in the hydrophobic pocket of the monomer/monomer interface but also is involved in a hydrogen bond to a strictly conserved glutamic acid at position 45, in the monomer partner of W20.

Other important residues include L17, R24, I51, I54, and I57. L17 is in both the monomer/monomer interface and the dimer/dimer interface. I54 is buried deep in the middle of the helix bundle in the dimer/dimer interface. R24 plays a role similar to that of R13 in protecting the hydrophobic core but only at the monomer/monomer interface. I57 is buried in the dimer/dimer interface but is more accessible to solvent than I54. L51 is sandwiched between the two tryptophans at positions 20 and 50. Residues V21 is at the very edge of the dimer/dimer interface and probably substitution of the valine by an alanine does not greatly affect the structure.

Expression and stability of δAg mutants. With this strategy in mind, the next question was to determine whether the mutant proteins were stably expressed. Vectors expressing the nine mutated forms of δAg-S and the corresponding nine forms of δAg-L were cotransfected into Huh7 cells, and the

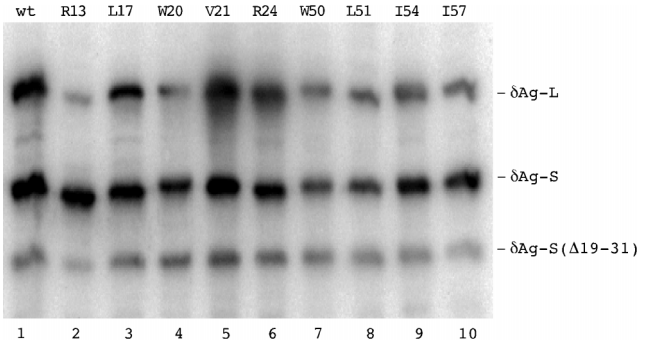

FIG. 2. Intracellular expression and accumulation of mutated forms of δAg-S and δAg-L. Huh7 cells were cotransfected with combinations of two plasmids that expressed different forms of δAg. Four days later, the proteins were assayed by electrophoresis and immunoblotting to detect δAg species. In each cotransfection, as an internal standard, we used a third plasmid which expressed δAg-S (Δ19–31). Relative to this standard, the cells received threefold-greater amounts of the two plasmids that express forms of δAg-S and δAg-L. As indicated for lanes 1 to 10, these two forms were either wild type (wt) or one of the nine mutants.

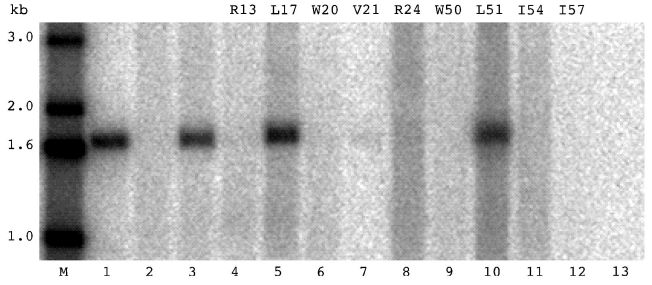

FIG. 3. Northern analysis to detect HDV replication supported in *trans* by δAg-S mutants. Huh7 cells were cotransfected with pTW148, which expresses 1.2× unit-length cDNA and has a frameshift in the δAg-S open reading frame, along with constructs expressing different forms of δAg-S. At 4 days after transfection, total cellular RNA was isolated and analyzed as described in Materials and Methods to detect antigenomic HDV RNA. Lanes 2 to 13 represent cells transfected with pTW148 alone (lane 2) or with constructs expressing wild-type δAg-S (lane 3), the indicated nine mutant constructs (lanes 4 to 12), or a construct expressing δAg-S(Δ19–31) (lane 13). Lane M shows 5′-labeled single-stranded DNA size markers. Lane 1 is 2 ng of 1.7-kb HDV cDNA.

levels of accumulation of the individual proteins assayed at 4 days by immunoblotting to detect delta protein. As an internal control, each cotransfection included a plasmid that expressed δAg-S(Δ19–31). Typical immunoblot results are shown in Fig. 2. From quantitation as presented in Table 1, it can be seen that for most cases somewhat less of the mutant protein accumulated. Furthermore, in most cases the levels of the large mutant were less than the corresponding mutant in small. In order to avoid artifacts due to such differences, in all subsequent cotransfection experiments we increased the input of plasmid DNA so that more equal amounts of protein might be accumulated.

***trans* support of genome replication by δAg-S mutants.** The most demanding test for a mutant δAg-S is whether it can support the replication of a mutated HDV genome that is unable to express wild-type δAg-S. This test was applied to the nine mutants of δAg-S. As shown in Fig. 3 and summarized in Table 2, only three of the nine mutants supported the synthesis and accumulation of HDV genomes. Two of these, L17 and V51, were equivalent to wild type. For reasons we do not understand, the third mutant, V21, reproducibly supported 10 to 20% accumulation of antigenomic RNA relative to wild type.

The six mutants that no longer supported genome replication were, according to the predictions, the six mutants most likely to be of importance for multimerization (Fig. 1B and C).

Dominant-negative inhibition of replication by δAg-S and δAg-L mutants. Previous studies have shown that like δAg-L, most altered forms of δAg-S lose the ability to support replication. Furthermore, relative to δAg-S, even low amounts can act as potent dominant-negative inhibitors (4, 15). When tested in the presence of wild-type δAg-S, none of the nine mutants were able to act as dominant-negative inhibitors, even when present in amounts approximately comparable to that of wild-type δAg-S (Fig. 4A).

As expected, L17, V21, and L51, which support replication, were not dominant-negative inhibitors. To distinguish between the other six mutants, we repeated the dominant-negative inhibition assays under conditions where each of the mutations was expressed not from δAg-S but from δAg-L. The results are shown in Fig. 4B and summarized in Table 2. As expected, L17, V21, and L51 were now dominant-negative inhibitors. Four of the other six mutants, R13, R24, I54, and I57, were dominant-negative inhibitors, indicating at least some ability to make protein interactions. In contrast, the remaining two mutants, W20 and W50, were inactive, suggesting that the efficiency of incorporation of these mutants into multimers is very low. Thus, we can now rank the nine mutations according to their effect on the assay of dominant-negative inhibition (Fig. 1C).

TABLE 1. Intracellular accumulation of mutated forms of δAg-S and δAg-L

Mutation in δAg species[a]	Accumulation (% of wt)[b]	
	δAg-S mutant	δAg-L mutant
R13	159	21
L17	65	40
W20	38	23
V21	61	112
R24	70	101
W50	32	32
L51	34	20
I54	59	35
I57	118	48

[a] As indicated in Fig. 1.
[b] Accumulation was determined from a series of triple cotransfections as in Fig. 2. Each value was then normalized relative to the accumulation of a common standard, after which the value for each mutant was expressed as a percentage of the accumulation for the corresponding δAg-S or δAg-L.

TABLE 2. Distinguishing properties of mutated forms of δAg-S and δAg-L

Mutation in δAg species[a]	Support of replication by δAg-S mutant[b]	Negative inhibition by δAg-L mutant[c]
R13	−	+
L17	+	+
W20	−	−
V21	+	+
R24	−	+
W50	−	−
L51	+	+
I54	−	+
I57	−	+
Δ19–31	−	−

[a] The mutations in δAg-S are as indicated in Fig. 1; Δ19–31 is described in Materials and Methods.
[b] Based on data as in Fig. 3.
[c] Based on data as in Fig. 4B.

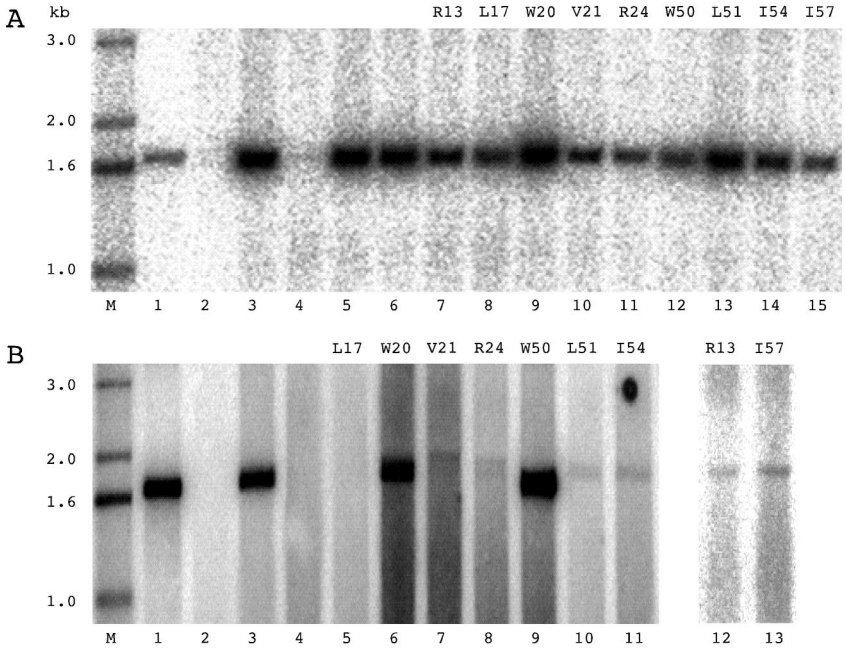

FIG. 4. Northern analysis to detect dominant-negative inhibition of HDV replication by δAg mutants. (A) Huh7 cells were cotransfected with plasmid pTW148, plasmid pDL444 (which expresses δAg-S), and a construct expressing one of the δAg-S mutants. At 4 days after transfection, total RNA was analyzed and detected as for Fig. 3. Lane M, 5′-labeled single-stranded DNA size markers; lane 1, 2 ng of 1.7-kb HDV cDNA; lane 2, cells transfected with pTW148 alone; lane 3, cells cotransfected with pTW148 and the construct expressing wild-type δAg-S; lanes 4 to 6, triple cotransfections with pTW148, the construct expressing wild-type δAg-S, and a construct expressing δAg-L (lane 4), δAg-S(Δ19–31) (lane 5), or δAg-L(Δ19–31) (lane 6); lanes 7 to 15, alanine mutants as indicated. (B) Experiments essentially as for panel A except that the mutations were expressed on δAg-L rather than δAg-S. Lanes 1 to 4, as in panel A; lanes 5 to 13, alanine mutants as indicated.

In the original predictions of importance in multimerization (Fig. 1B), W20 and W50 were in the top three. Thus, we would again conclude that the predictions are in good agreement with the in vivo data.

Coassembly of δAg-S and δAg-L mutants. Our next test was whether mutants expressed on δAg-S would, in the presence of the envelope proteins of HBV, be coassembled by wild-type δAg-L and released as virus-like particles. We observed that each of the nine mutants expressed on δAg-S could be coassembled (Fig. 5). Quantitation of these data showed that the efficiencies were within a factor of 3 of that for wild-type δAg-S (Table 3). We do not consider these as significant differences. Furthermore, the molar ratio of mutant δAg-S to wild-type δAg-L in the released particles was less than 1 (Table 3). This was also true when the amount of mutant δAg-S expressed within the cell was increased fourfold (data not shown; see also reference 22). One interpretation of these data would be that coassembly efficiency reflects not multimerization ability but only dimerization, and that this dimerization was not affected by the nine mutations.

However, the data and their interpretation became more complex when we used two variants of the coassembly assay. We now asked whether each mutant, as expressed on δAg-L, could coassemble either the wild-type δAg-S or the corresponding mutant as expressed on δAg-S. The quantitation of these data (Table 3) reveals major differences in coassembly efficiency. Consider first the coassembly of wild-type δAg-S. It can be seen that with the exception of V21 and R24, the δAg-L mutants demonstrated a reduction in coassembly efficiency; for I57, it was as much as 40-fold. Next consider the coassembly of mutant δAg-S by the corresponding mutant in δAg-L. Again V21 and R24 were the same as for wild type, but for all the others, the reductions in efficiency were even greater than in the previous experiment.

In summary, these three forms of the coassembly assay provide different answers in terms of the effects of the mutations. Furthermore, none of these effects are as predicted from the crystal structure (Fig. 1B). However, as considered in Discussion, both the different answers and the disagreement with predictions might be largely a consequence of the coassembly assay, with its additional dependence on interactions of the δAg-L with the envelope proteins of HBV.

Immunoaffinity purification of complexes formed between δAg-S(FLAG) and δAg-S or δAg-L mutants. Another way to assay the interactions between δAg species is via immunoaffinity. We expressed within transfected cells both δAg-S (FLAG) and each of the mutants of either δAg-S or δAg-L. As shown in Fig. 6, we were able to demonstrate the formation of

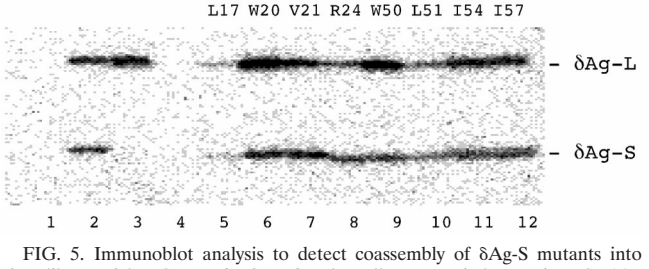

FIG. 5. Immunoblot analysis to detect coassembly of δAg-S mutants into virus-like particles. Cotransfection of Huh7 cells was carried out using pSV45H (to express the envelope proteins of HBV) along with pDL445 (to express wild-type δAg-L) and constructs expressing mutants of δAg-S. As described in Materials and Methods, virus-like particles released by the transfected cells were subsequently collected and assayed by electrophoresis and immunoblotting to detect δAg species. Lane 1, particles from cells expressing wild-type δAg-S in the absence of δAg-L; lane 2, both δAg-S and δAg-L; lane 3, δAg-S(Δ19–31) and δAg-L; lane 4, δAg-S and δAg-L(Δ19–31); lanes 5 to 12, wild-type δAg-L and the indicated mutants in δAg-S. The mobilities of δAg-L and δAg-S are indicated at the right.

TABLE 3. Effect of mutations on efficiency of coassembly into virus-like particles

Mutation in δAg species[a]	Pairing of δAg-S and δAg-L used in cotransfection[b]								
	δAg-S mutant/δAg-L			δAg-S/δAg-L mutant			δAg-S mutant/δAg-L mutant		
	I	O	O/I	I	O	O/I	I	O	O/I
R13	1.6	0.45	0.29	2.2	0.16	0.072	11	0.63	0.059
L17	1.9	1.0	0.54	3.1	0.54	0.17	2.8	0.050	0.017
W20	0.64	0.32	0.50	2.1	0.17	0.079	4.4	0.0070	0.0010
V21	1.3	0.82	0.63	0.35	0.35	1.0	0.57	0.25	0.44
R24	1.5	1.2	0.81	0.34	0.46	1.3	0.77	0.28	0.36
W50	0.77	0.27	0.35	1.2	0.037	0.030	2.0	0.037	0.019
L51	1.2	0.94	0.75	1.6	0.25	0.16	4.9	0.050	0.010
I54	2.1	0.64	0.29	0.86	0.052	0.060	4.2	0.050	0.011
I57	3.3	0.75	0.22	3.4	0.030	0.0080	9.1	0.0090	0.00090

[a] As described in Fig. 1.
[b] The cotransfections used in these coassembly experiments involved a plasmid expressing the envelope proteins of HBV along with plasmids expressing the forms of δAg-S and δAg-L, either wild type or mutant, as indicated. Other details are described in Materials and Methods. The immunoblot analyses were quantitated and used to deduce the values indicated for the ratio of δAg-S form to δAg-L in transfected cells (I) or in virus-like particles (O). Also shown is the ratio O/I. As a positive control, the coassembly of wild-type δAg-S by wild-type δAg-L gave average values for I, O, and O/I of 1.6, 0.44, and 0.30, respectively.

these complexes. As an indicator of the specificity of these complexes, we also expressed in these cells the protein δAg-S (Δ19–31), which is known to be unable to make dimers (15). As shown in Fig. 6, this protein was present in the total sample but virtually absent from the fraction of bound protein.

We quantitated these data (Table 4) to determine the effect of each of the mutations on the ability of both δAg-S and δAg-L to make complexes with δAg-S(FLAG). From an average of the effects on both δAg-S and δAg-L, we deduced a hierarchy of importance, as summarized in Fig. 1C. This is not exactly the same as the predicted hierarchy presented in Fig. 1B, but it is very close.

Ability of δAg-S mutants to enhance the accumulation of processed HDV RNA circles. In conclusion, these assays were carried out as a negative control, that is, to determine whether the mutagenesis of δAg-S interfered with a biological property that does not depend on dimerization and multimerization.

Previous studies have shown that when nonreplicating multimeric forms of HDV RNA are expressed in cells, there can be processing of these RNA by the HDV ribozymes and, somehow, the formation of unit-length RNA circles (14). Furthermore, the simultaneous expression of δAg-S or δAg-L is known to increase the accumulation of such circles as much as 16-fold (8, 14). Thus, our strategy was to cotransfect cells with the mutant forms of δAg-S along with a construct that can express multimers of a deleted form of HDV RNA. As previously shown, this deleted RNA can be processed to form a unit-length circle of about 1,200 nucleotides (14). We assayed the accumulation of unit-length circles at days 2 and 4 after transfection. Our results (Table 5) indicate that each of the mutants produced an 8- to 25-fold increase in accumulation relative to expression in the absence of any form of δAg-S. Thus, they demonstrated just as much of this particular biological activity as did wild-type δAg-S or the deleted form of δAg-S, Δ19–31, which does not dimerize (15). Incidentally, this is the first reported evidence that this biological property of δAg is independent of dimerization.

DISCUSSION

The aim of this study was to evaluate predictions for the dimerization and multimerization of δAg. These predictions were based on intermolecular interactions detected in the crystal structure of the domain of aa 12 to 60 on the δAg (29). We considered mutagenesis to alanine at nine sites that were (i) conserved between different isolates of HDV and (ii) predicted to be important for dimerization and/or multimerization (Fig. 1A). We tested these mutants in the context of both full-length δAg-S and δAg-L, via biological assays, using transfected cells.

The top six mutants of δAg-S, in terms of their predicted

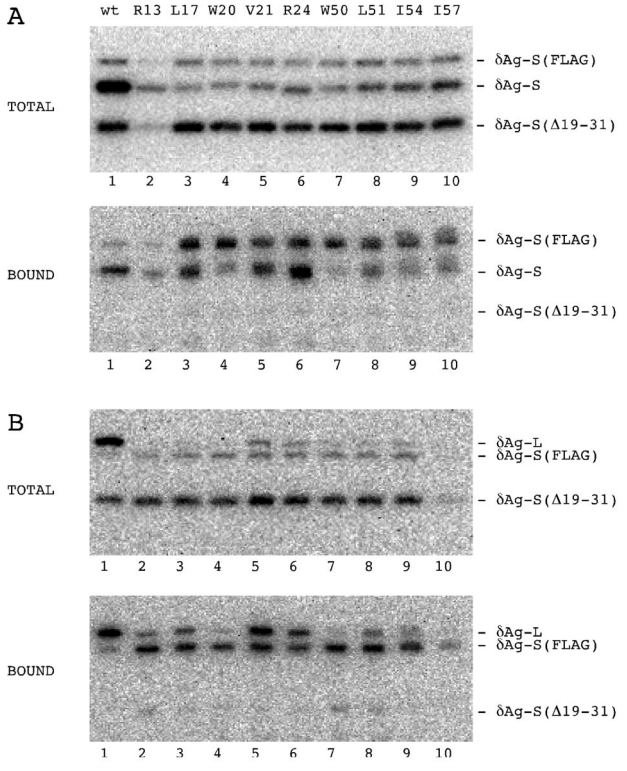

FIG. 6. Immunoblot analysis to detect complexes formed between δAg-S (FLAG) and mutant forms of δAg-S and δAg-L. (A) Huh7 cells were cotransfected with plasmids pPB102 [expressing δAg-S(Δ19–31)] and pPB105 [expressing δAg-S(FLAG)], along with pTW198 (expressing wild-type δAg-S; lane 1) or plasmids expressing the indicated mutants of δAg-S (lanes 2 to 10). At 5 days after transfection, we isolated that protein which bound via the FLAG epitope to an immunoaffinity column. Samples of total and bound protein were assayed by gel electrophoresis and immunoblotting to detect all forms of δAg. The three electrophoretic forms of δAg-S are indicated at the right. Note that δAg-S(Δ19–31) acts as a negative control which fails to bind to δAg-S(FLAG). (B) Experiments essentially as for panel A except that the mutations were expressed on δAg-L rather than δAg-S. That is, we used pTW199 (expressing wild-type δAg-L; lane 1) or plasmids expressing the indicated mutants of δAg-L (lanes 2 to 10).

TABLE 4. Effect of mutations on ability to form complexes with δAg-S(FLAG)

Mutation in δAg species[a]	Pairing of δAg-S and δAg-L with δAg-S(FLAG)[b]					
	δAg-S mutant/δAg-S (FLAG)			δAg-L mutant/δAg-S (FLAG)		
	T	B	B/T	T	B	B/T
R13	5.9	2.2	0.37	0.31	0.29	0.96
L17	0.91	0.88	0.97	0.39	0.47	1.2
W20	1.2	0.33	0.27	0.36	0.13	0.36
V21	1.6	1.2	0.76	0.83	1.4	1.7
R24	2.4	1.5	0.65	0.81	0.98	1.2
W50	1.4	0.27	0.19	0.48	0.11	0.22
L51	1.6	0.69	0.43	0.46	0.28	0.61
I54	2.2	0.56	0.25	0.52	0.28	0.53
I57	2.3	0.67	0.29	0.73	0.23	0.31

[a] As described in Fig. 1.

[b] The cotransfections used in these immunoaffinity experiments involved plasmids expressing the mutant forms of δAg-S or δAg-L, along with expression of δAg-S(FLAG) and δAg-S(Δ19–31). Other details are described in Materials and Methods. The immunoblot data shown in Fig. 6 were quantitated and used to deduce the values indicated for the ratio of δAg-S mutant or δAg-L mutant to δAg-S(FLAG) in the intact transfected cells (T) or in the fraction immunoaffinity purified from these cells (B). Also shown is the ratio B/T. As positive controls, the immunoaffinity data for wild-type δAg-S or δAg-L to δAg-S(FLAG) gave values for T, B, and B/T of 9.9, 3.6, and 0.37 and of 17, 7.3, and 0.42, respectively.

importance for dimerization/multimerization (Fig. 1B), were the ones that could no longer support replication (Fig. 3). To this extent these results followed the predictions. We also note that four of these mutations were of hydrophobic amino acids predicted to be important in the interactions that form the dimer (Fig. 1B).

Another consistent correlation was obtained when the nine mutants, as expressed on δAg-L, were tested as dominant-negative inhibitors of replication, as supported by wild-type δAg-S (Fig. 4B). Seven mutants were inhibitors. Three of these (L17, V21, and L51) were the same as those that when expressed on δAg-S were able to support replication. However, it was unexpected that the four additional mutants (R13, I54, R24, and I57) were dominant-negative inhibitors. One explanation might be that, as for mutants in the nucleocapsid of tomato spotted wilt virus (25), the heterotypic interaction between the mutant and the wild type (as in the dominant-negative inhibition assay) could be stronger than the homotypic interaction between two mutants (as in the support of replication assay).

Results of the dominant-negative inhibition assays also showed that mutations of W20 and W50 were the most potent of the nine amino acid mutations tested (Fig. 1C and 3B). This ranking also agrees with the predictions based on the crystal structure (Fig. 1B). It is important to note that it was originally suggested from examination of the structure that dimerization was stabilized by the hydrophobic interactions of I16, L17, and W20 from one monomer to W50, L51, and I54 on a second monomer, and vice versa (29). Therefore, the present data not only support this interpretation but also indicate that the two tryptophans, W20 and W50, are critical residues.

In contrast to the above good correlations between prediction and experiment, there were also less favorable situations. First, we found that none of the mutants, when expressed on δAg-S, was a dominant-negative inhibitor (Fig. 4A; Table 2). In contrast, when expressed on δAg-L, we did observe inhibition for L17, V21, and L51 (Fig. 4B; Table 2), and this was as expected, since these, as expressed on δAg-S, were able to support genome replication (Fig. 3; Table 2). We speculate that for these three mutations, as expressed on δAg-S, there was insufficient structural difference from wild-type δAg-S to produce any inhibition.

A second discrepancy arose when we tested the mutants in three different assays of protein coassembly into virus-like particles in the presence of the envelope proteins of HBV (Table 3). The first assay was for the coassembly by wild-type δAg-L of mutants expressed on δAg-S. Each mutant was coassembled as efficiently as wild-type δAg-S. This was unexpected since six of these mutants could neither support replication (Fig. 3) nor act as dominant-negative inhibitors (Fig. 4A). Since we consider that the coassembly assay detects dimerization but not multimerization, it may be unable to distinguish functional from nonfunctional dimers. Therefore, one interpretation is that the six mutants were able to make only nonfunctional dimers. In addition, it must be remembered that the coassembly assay involves more than just interactions between δAg species; there are also essential interactions with the envelope proteins of the helper virus in order to achieve assembly into the virus-like particles (9). Moreover, recent studies show that δAg-L is significantly more hydrophobic than δAg-S, and that some of the δAg-L species have to undergo isoprenylation as a prerequisite for interaction with the envelope proteins of the helper virus (7, 19). These factors might contribute to the diversity of results obtained for the coassembly by mutant δAg-L, of wild-type δAg-S, or of mutant δAg-S (Table 3).

Our interpretation of the subset of the present in vivo studies specifically concerned with the support of genome replication and the dominant-negative inhibition is that the essential interactions between the δAg species are not random but ordered and consistent with the predictions based on the crystal structure for the 12-60 peptide. Independent of these studies, from application of an immunoaffinity strategy, we obtained direct in vivo evidence for the ability of the mutated forms of δAg-S and δAg-L to make complexes with a form of δAg-S containing at its N terminus a FLAG epitope. These data show that all the mutated forms were able to bind to the tagged protein (Fig. 6; Table 5) and thus were at least able to form dimers. (Incidentally, this agrees with the results obtained by coassembly [Fig. 5].) Furthermore, analysis of the quantitation of these data (Table 4) reveals that the predicted hierarchy (Fig. 1B) is close to the directly observed values (Fig. 1C). This immunoaffinity strategy also allows us to begin to address the question of in vivo complexes larger than dimers. The wild-type forms of δAg-S and δAg-L made complexes with the

TABLE 5. Accumulation of processed HDV RNA in the presence of mutated forms of δAg-S

Mutation in δAg-S species[a]	Accumulation of processed RNA (%)[b]	
	Day 2	Day 4
No protein	4	12
L17	132	86
W20	232	129
V21	91	91
R24	141	114
W50	165	187
L51	136	213
I54	143	113
I57	124	124
Δ19–31	39	133

[a] The mutations in δAg-S are as indicated in Fig. 1; Δ19–31 is described in Materials and Methods.

[b] Accumulation of unit-length genomic HDV RNA was determined by Northern analyses, and the values are expressed as a percentage of that achieved in the presence of wild-type δAg-S.

tagged δAg-S that on average were at least greater than tetramers (Fig. 6, lane 1; Table 4, footnotes). Further studies using the same strategy, indicate complexes of at least decamers (data not shown). It will be necessary to determine to what extent these multimers are ordered. At this stage there is no in vivo evidence to suggest that δAg can behave like the core protein of the helper virus, HBV, and form ordered multimeric capsid structures (27). In contrast, we have already seen from electrophoretic analyses under nondenaturing conditions that within transfected cells δAg can become associated with high-molecular-weight complexes (6). Maybe δAg, like other proteins when expressed to high levels in bacterial or mammalian cells, can produce multimeric aggregates that are disordered (10). Furthermore, there may be additional components in the δAg complexes and some of the δAg interactions may be indirect. After all, we know that δAg species have to interact with HDV RNAs and, during assembly, interact with the envelope proteins of the helper virus. In addition, the δAg can also interact with host proteins; others have described candidate host protein interactors, namely, nucleolin (16) and delta-interacting protein A (1).

ACKNOWLEDGMENTS

This work was supported by grants AI-26522 and CA-06927 from the NIH and by an appropriation from the Commonwealth of Pennsylvania.

Thanks go to Cheng-Ming Chiang for advice regarding immunoaffinity purification and to Don Ganem for the plasmid pSV45H. We also thank Severin Gudima, William Mason, and Glenn Rall for constructive comments on the manuscript.

REFERENCES

1. **Brazas, R., and D. Ganem.** 1996. A cellular homolog of hepatitis delta antigen: implications for viral replication and evolution. Science **274:**90–94.
2. **Chang, F. L., P. J. Chen, S. J. Tu, M. N. Chiu, C. J. Wang, and D. S. Chen.** 1991. The large form of hepatitis δ antigen is crucial for the assembly of hepatitis δ virus. Proc. Natl. Acad. Sci. USA **88:**8490–8494.
3. **Chang, M.-F., S. C. Baker, L. H. Soe, T. Kamahora, J. G. Keck, S. Makino, S. Govindarajan, and M. M. C. Lai.** 1988. Human hepatitis delta antigen is a nuclear phosphoprotein with RNA binding activity. J. Virol. **62:**2403–2410.
4. **Chao, M., S.-Y. Hsieh, and J. Taylor.** 1991. The antigen of hepatitis delta virus: examination of in vitro RNA-binding specificity. J. Virol. **65:**4057–4062.
5. **Chiang, C.-M., H. Ge, Z. Wang, A. Hoffmann, and R. G. Roeder.** 1993. Unique TATA-binding protein-containing complexes and cofactors involved in transcription by RNA polymerases II and III. EMBO J. **12:**2749–2762.
6. **Dingle, K., G. Moraleda, V. Bichko, and J. Taylor.** 1998. Electrophoretic analysis of the ribonucleoproteins of hepatitis delta virus. J. Virol. Methods **75:**199–204.
7. **Glenn, J. S.** 1995. Prenylation and virion morphogenesis, p. 83–94. *In* G. Dinter-Gottlieb (ed.), The unique hepatitis delta virus. R. G. Landes Co., Austin, Tex.
8. **Jeng, K.-S., P.-Y. Su, and M. M. C. Lai.** 1996. Hepatitis delta antigen enhances the ribozyme activities of hepatitis delta virus RNA in vivo. J. Virol. **70:**4205–4209.
9. **Jenna, S., and C. Sureau.** 1999. Mutations in the carboxyl-terminus domain of the small hepatitis B virus envelope protein impair the assembly of hepatitis delta virus particles. J. Virol. **73:**3351–3358.
10. **Kazantsev, A., E. Preisinger, A. Dranovsky, D. Goldgaber, and D. Housman.** 1999. Insoluble detergent-resistant aggregates form between pathological and nonpathological length of polyglutamine in mammalian cells. Proc. Natl. Acad. Sci. USA **96:**11404–11409.
11. **Kuo, M. Y.-P., M. Chao, and J. Taylor.** 1989. Initiation of replication of the human hepatitis delta virus genome from cloned DNA: role of delta antigen. J. Virol. **63:**1945–1950.
12. **Kuo, M. Y.-P., J. Goldberg, L. Coates, W. Mason, J. Gerin, and J. Taylor.** 1988. Molecular cloning of hepatitis delta virus RNA from an infected woodchuck liver: sequence, structure, and applications. J. Virol. **62:**1855–1861.
13. **Laemmli, U. K.** 1970. Cleavage of structural proteins during the assembly of the head of bacteriophage T4. Nature **227:**680–685.
14. **Lazinski, D. W., and J. M. Taylor.** 1994. Expression of hepatitis delta virus RNA deletions: *cis* and *trans* requirements for self-cleavage, ligation, and RNA packaging. J. Virol. **68:**2879–2888.
15. **Lazinski, D. W., and J. M. Taylor.** 1993. Relating structure to function in the hepatitis delta virus antigen. J. Virol. **67:**2672–2680.
16. **Lee, C.-H., S. C. Chang, C.-J. Chen, and M.-F. Chang.** 1998. The nucleolin binding activity of hepatitis delta antigen is associated with nucleolus targeting. J. Biol. Chem. **273:**7650–7656.
17. **Luo, G., M. Chao, S.-Y. Hsieh, C. Sureau, K. Nishikura, and J. Taylor.** 1990. A specific base transition occurs on replicating hepatitis delta virus RNA. J. Virol. **64:**1021–1027.
18. **Makino, S., M. F. Chang, C. K. Shieh, T. Kamahora, D. M. Vannier, and M. M. C. Lai.** 1987. Molecular cloning and sequencing of a human hepatitis delta (δ) virus RNA. Nature **329:**343–346.
19. **Moraleda, G., S. Seeholzer, V. Bichko, R. Dunbrack, J. Otto, and J. Taylor.** 1999. Unique properties of the large antigen of hepatitis delta virus. J. Virol. **73:**7147–7152.
20. **Nakabayashi, H., K. Taketa, K. Miyano, T. Yamane, and J. Sato.** 1982. Growth of human hepatoma cell lines with differentiated functions in chemically defined medium. Cancer Res. **42:**3858–3863.
21. **Rozzelle, J., J.-G. Wang, D. Wagner, B. Erickson, and S. Lemon.** 1995. Self-association of a synthetic peptide from the N terminus of the hepatitis delta virus protein into an immunoreactive alpha-helical multimer. Proc. Natl. Acad. Sci. USA **92:**382–386.
22. **Ryu, W.-S., M. Bayer, and J. Taylor.** 1992. Assembly of hepatitis delta virus particles. J. Virol. **66:**2310–2315.
23. **Ryu, W. S., H. J. Netter, M. Bayer, and J. Taylor.** 1993. Ribonucleoprotein complexes of hepatitis delta virus. J. Virol. **67:**3281–3287.
24. **Taylor, J. M.** 1999. Human hepatitis delta virus: structure and replication of the genome. Curr. Top. Microbiol. Immunol. **239:**108–122.
25. **Uhrig, J. F., T.-R. Soellick, C. J. Minke, C. Phillipp, J.-W. Kellmann, and P. H. Schreier.** 1999. Homotypic interaction and multimerization of nucleocapsid protein of tomato spotted wilt tospovirus: identification and characterization of two interacting domains. Proc. Natl. Acad. Sci. USA **96:**55–60.
26. **Wu, T.-T., H. J. Netter, D. W. Lazinski, and J. M. Taylor.** 1997. Effects of nucleotide changes on the ability of hepatitis delta virus to transcribe, process, and accumulate unit-length, circular RNA. J. Virol. **71:**5408–5414.
27. **Wynne, S. A., R. A. Crowther, and A. G. Leslie.** 1999. The crystal structure of the human hepatitis B virus capsid. Mol. Cell **3:**771–780.
28. **Xia, Y.-P., C.-T. Yeh, J.-S. Ou, and M. M. C. Lai.** 1992. Characterization of nuclear targeting signal of hepatitis delta antigen: nuclear transport as a protein complex. J. Virol. **66:**914–921.
29. **Zuccola, H. J., J. E. Rozzelle, S. M. Lemon, B. W. Erickson, and J. M. Hogle.** 1998. Structural basis of the oligomerization of hepatitis delta antigen. Structure **6:**821–830.